CHEMISTRY OF MATERIALS

Article

pubs.acs.org/cm

Revealing the Charge Transport Mechanism in Polymerized Ionic Liquids: Insight from High Pressure Conductivity Studies

Zaneta Wojnarowska,*[,†,‡,§] Hongbo Feng,[⊥] Mariana Diaz,[¶] Alfredo Ortiz,[¶] Inmaculada Ortiz,[¶] Justyna Knapik-Kowalczuk,[‡,§] Miguel Vilas,[□] Pedro Verdía,[□] Emilia Tojo,[□] Tomonori Saito,[†] Eric W. Stacy,[●] Nam-Goo Kang,[⊥] Jimmy W. Mays,[†,⊥] Danuta Kruk,[■] Patryk Wlodarczyk,[○] Alexei P. Sokolov,[⊥,●] Vera Bocharova,[†] and Marian Paluch[‡,§]

[†]Chemical Sciences Division, Oak Ridge National Laboratory, Oak Ridge, Tennessee 37831, United States

[‡]Institute of Physics, University of Silesia, Uniwersytecka 4, Katowice 40-007, Poland

[§]Silesian Center for Education and Interdisciplinary Research, 75 Pulku Piechoty 1A, Chorzow 41-500, Poland

[⊥]Department of Chemistry, University of Tennessee, Knoxville, Tennessee 37996, United States

[¶]Chemical and Biomolecular Engineering Department, University of Cantabria, Avenida de los Castros s/n, Santander 39005, Spain

[□]Organic Chemistry Department, University of Vigo, Marcosende, Vigo 36210, Spain

[■]Faculty of Mathematics and Computer Science, University of Warmia and Mazury in Olsztyn, Sloneczna 54, Olsztyn PL-10710, Poland

[○]Institute of Non-Ferrous Metals, Sowinskiego 5, Gliwice 44-100, Poland

[●]Department of Physics and Astronomy, University of Tennessee, Knoxville, Tennessee 37996, United States

Supporting Information

ABSTRACT: Polymerized ionic liquids (polyILs), composed mostly of organic ions covalently bonded to the polymer backbone and free counterions, are considered as ideal electrolytes for various electrochemical devices, including fuel cells, supercapacitors, and batteries. Despite large structural diversity of these systems, all of them reveal a universal but poorly understood feature: a charge transport faster than the segmental dynamics. To address this issue, we studied three novel polymer electrolyte membranes for fuel cells as well as four single-ion conductors, including highly conductive siloxane-based polyIL. Our ambient and high pressure studies revealed fundamental differences in the conducting properties of the examined systems. We demonstrate that the proposed methodology is a powerful tool to identify the charge transport mechanism in polyILs in general and thereby contribute to unraveling the microscopic nature of the decoupling phenomenon in these materials.

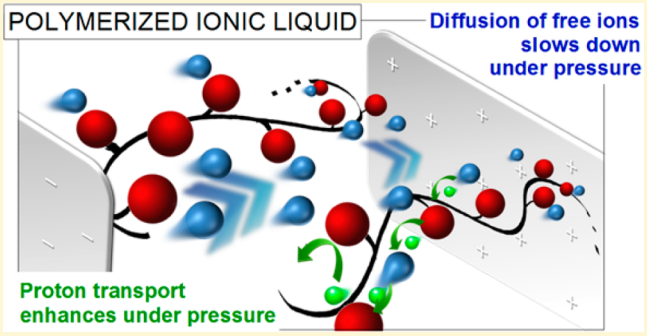

INTRODUCTION

Efficient generation and utilization of energy has become one of the greatest challenges of our time. This in turn creates a growing demand for various types of energy storage devices in household and in industry. Therefore, a significant research effort during the past decade has been focused on development of new functional materials for diverse energy storage applications.[1−3] The family of polymerized ionic liquids (polyILs), combining unique futures of ionic liquids with the outstanding mechanical properties of polymers, might offer an ideal solution for these purposes. An almost unlimited combination of cations, anions, and polymer chains provides the possibility to design numerous combinations of chemically distinct polyIL materials of technological importance.[4] The rational design of polyILs requires fundamental understanding of the microscopic parameters controlling their macroscopic properties, including conductivity. For this reason, in recent years, much effort has been dedicated to fundamental understanding of the charge transport mechanism in polyILs.

It has been found that in contrast to low-molecular weight aprotic ionic liquids (composed solely of ions), where the charge transport is fully controlled by viscosity,[5] the ion mobility in polyILs can be strongly decoupled from segmental (structural) dynamics.[6−11] As a consequence, the classical Walden theory predicting similar temperature dependence for the dc conductivity and mass diffusion (fluidity), fails for macromolecular conductors. In particular, when the segmental mobility slows due to the glassy freezing, the rate of ion motions in

Received: April 23, 2017
Revised: September 2, 2017
Published: September 5, 2017

DOI: 10.1021/acs.chemmater.7b01658
Chem. Mater. XXXX, XXX, XXX−XXX

polyILs can be many orders of magnitude faster,[12] resulting in dc conductivity significantly higher than the conductivity in an ideally coupled system (at $T_g \sim 10^{-14}$ to 10^{-15} S/cm).[13−15]

From a fundamental point of view, two types of conductivity mechanisms have been recognized to decouple charge transport from segmental dynamics in polyILs. It was hypothesized that the decoupling can be caused by a frustration in chain packing (free volume) that enables ion diffusion even when the segmental dynamics are frozen. In such case, the positive or negative species can freely move through the holes in the matrix formed by counterions covalently bonded to the polymer backbone. The decoupling phenomenon is also known for polymer electrolyte membranes for fuel cells obtained by polymerization of protic ionic liquids (PILs) and in low-molecular PILs themselves.[16] In these cases, the difference in time scale of conductivity relaxation and segmental dynamics is usually attributed to the proton transfer mechanism through the H-bonded network and thereby does not require diffusion of entire molecular units (vehicles).[17−19] According to the literature reports, two mechanisms of proton transport can be distinguished. Namely, so-called Grotthuss picture, was originally proposed to explain high conductivity of water, where the protonic defect is moved from one electrode to another while a given proton is transferred only between two neighboring molecules; and the other case where the same proton is sequentially transferred within hydrogen bonds from one "vehicle" to the other. Importantly, among the computational studies of phosphoric acid and imidazolium-based compounds,[20] no clear experimental verification of the Grotthuss mechanism has been provided so far. Additionally, in many protic ionic systems, an efficient proton transport does not occur, although it was expected on the basis of chemical composition.[21]

Because in disordered ionic polymers there are many potential charge carriers, it becomes a challenge to clearly define the dominating mechanism.[22] We emphasize that the usual conductivity measurements do not provide any microscopic details of the conductivity mechanism, being critical for understanding their behavior in fuel cell and battery applications.

In this paper, we investigate the conducting properties of seven polymerized ionic liquids that can be classified in three categories: aprotic polycations, protic polyanions, and polymer blends (see Table 1 for chemical structures). To reveal the charge transport mechanism in these materials, we employ high pressure conductivity measurements. We show that isothermal compression offers a unique possibility to recognize the dominating charge transport mechanisms as well as to control the conducting properties of polymeric ILs, both being crucial in their potential electrochemical applications. We demonstrate that the proton transfer mechanism can be easily distinguished from vehicle conduction in any low-molecular weight or macromolecular ionic system.

Table 1. Chemical Structures of Investigated polyILs

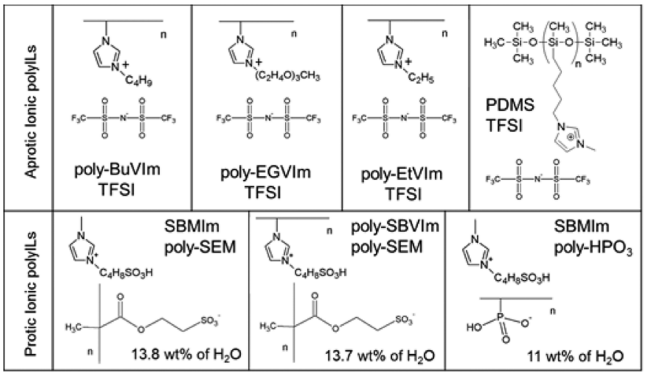

EXPERIMENTAL SECTION

In this study, we investigated three novel protic polymerized ionic liquids obtained by UV polymerization of corresponding monomers: (i) polyanion 1-butylsulfonate-3-methylimidazolium poly-(2-sulfethylmetacrylate) (SBMIm poly-SEM), (ii) polymer blend poly-(1-butylsulfonate-3-vinylimidazolium) poly-(2-sulfethylmetacrylate) (poly-SBVIm poly-SEM)-polyanion, and (iii) 1-butylsulfonate-3-vinylimidazolium poly-(vinylphosphonic acid) (SBMIm poly-HPO_3).

Additionally, we studied the charge transport mechanism in the group of aprotic polyILs: (i) poly-(1-ethyl-3-vinylimidazolium bis-(trifluoromethylsulfonyl)imide) (poly-EtVIm TFSI), (ii) poly-(*N*-vinyl diethylene glycol ethyl methyl ether imidazolium) bis-(trifluoromethylsulfonyl)imide (poly-EGIm TFSI), (iii) poly-(1-butyl-3-vinylimidazolium bis-(trifluoromethylsulfonyl)-imide) (poly-BuVIm TFSI), and (iv) polymethylhydrosiloxane-*graft*-5-imidazolium-1-pentene bis (trifluoromethane) sulfonamide (PDMS TFSI).

The synthesis procedures of poly-EtVIm TFSI, poly-BuVIm TFSI, and poly-EGIm TFSI are provided in refs 23 and 24.

Chemicals. 1-Methylimidazole (Acros Organics, 99%), 1-vinylimidazole (Sigma-Aldrich, ≥99%), 1,4-butane sultone (Acros Organics, 99+%), acetonitrile (Sigma-Aldrich, ACS reagent, ≥99%), and 2-sulfethyl methacrylate (Polysciences, >90%) were obtained from the commercial suppliers and used without any pretreatment.

General Procedure for the Synthesis of the 1-Alkyl-3-Butylsulfonate Imidazolium Zwitterions.

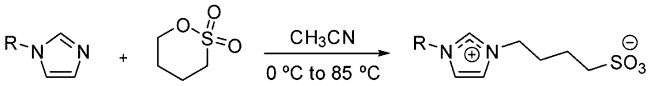

Synthesis of 1-Butylsulfonate-3-methylimidazolium Zwitterion. 1-Methylimidazole (1.00 mL, 12.5 mmol, 1.00 equiv) was dissolved in CH_3CN (8 mL) and cooled to 0 °C with an ice bath. 1,4-Butane sultone (1.28 mL, 12.5 mmol, 1.00 equiv) was added dropwise, and the mixture was allowed to stir at 0 °C for 10 min. Then, it was stirred at 85 °C under reflux for 3 days. It was then cooled to −20 °C, and the resulting precipitate was filtered and dried under high vacuum. 1-Butylsulfonate-3-methylimidazolium was obtained as a white solid (2.29 g, 84% yield). ^{1}H NMR (400 MHz, D_2O) δ 8.77 (s, 1-H, H-2), 7.53 (s, 1H, H-5*), 7.47 (s, 1H, H-4*), 4.28 (t, J = 6.9 Hz, 2H, NCH_2), 3.92 (s, 3H, NCH_3), 2.97 (t, J = 7.6 Hz, 2H, N-$(CH_2)_3CH_2SO_3$), 2.16−1.97 (m, 2H, N-$(CH_2)_2CH_2$), 1.83−1.72 (m, 2H, NCH_2CH_2); ^{13}C NMR (101 MHz, D_2O) δ 136.0 (C-2), 123.7 (C-5*), 122.2 (C-4*), 50.0 (N-$(CH_2)_3CH_2SO_3$), 48.9 (NCH_2), 35.7 (NCH_3), 28.1 (NCH_2CH_2), 20.9 (N-$(CH_2)_2CH_2$).[25]

Synthesis of 1-Butylsulfonate-3-vinylimidazolium Zwitterion. 1-Butylsulfonate-3-vinylimidazolium was prepared employing the same general synthetic method described for the synthesis of 1-butylsulfonate-3-methylimidazolium, employing 1-vinylimidazole instead of 1-methylimidazole, and obtained as a white solid (1.61 g, 63% yield). ^{1}H NMR (400 MHz, D_2O) δ 9.05 (s, 1H, H-2), 7.74 (d, J = 1.7 Hz, 1H, H-5*), 7.57 (d, J = 1.6 Hz, 1H, H-4*), 7.10 (dd, J = 15.6, 8.7 Hz, 1H, NC*H*=CH_2), 5.76 (dd, J = 15.6, 2.6 Hz, 1H, NCH=C*H*H), 5.38 (dd, J = 8.7, 2.6 Hz, 1H, NCH=CH*H*), 4.26 (t, J = 7.0 Hz, 2H, NCH_2), 2.92 (t, J = 7.6 Hz, 2H, N-$(CH_2)_3CH_2SO_3$), 2.16−1.87 (m, 2H, N-$(CH_2)_2CH_2$), 1.90−1.55 (m, 2H, NCH_2CH_2); ^{13}C NMR (101 MHz, D_2O) δ 134.5 (C-2), 128.2 (C-5*), 122.7 (C-4*), 119.5 (NCH=CH_2), 109.2 (NCH=CH_2), 49.9 (N-$(CH_2)_3CH_2SO_3$), 49.2 (NCH_2), 27.9 (NCH_2CH_2), 20.8 (N-$(CH_2)_2CH_2$).[26]

DOI: 10.1021/acs.chemmater.7b01658
Chem. Mater. XXXX, XXX, XXX−XXX

General Procedure for the Synthesis of the Sulfethyl Methacrylate Ionic Liquids.

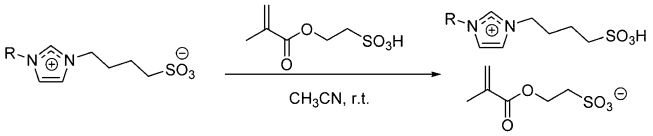

Synthesis of 1-Butylsulfonate-3-methylimidazolium 2-Sulfethylmetacrylate. 2-Sulfethyl methacrylate (1.84 g, 9.5 mmol, 1.00 equiv) was dissolved in CH_3CN and added over 1-butylsulfonate-3-methylimidazolium (2.29 g, 10.5 mmol, 1.10 equiv). The mixture was stirred at rt overnight and then filtered to remove the unreacted excess of the zwitterion. The organic phase was collected, and the solvent was evaporated under reduced pressure at room temperature to avoid product decomposition. The resulting IL was dried under high vacuum to obtain 1-butylsulfonic-3-methylimidazolium 2-sulfethyl methacrylate as a viscous ionic liquid (3.91 g, 99% yield). ^{1}H NMR (400 MHz, D_2O) δ 8.59 (s, 1H, H-2), 7.35 (d, J = 1.5 Hz, 1H, H-4*), 7.29 (d, J = 1.2 Hz, 1H, H-5*), 6.01 (d, J = 0.9 Hz, 1H, CH_3C-(C*H*H)-$CO_2CH_2CH_2SO_3$), 5.57 (d, J = 1.4 Hz, 1H, CH_3C-(C*H*H)-$CO_2CH_2CH_2SO_3$), 4.37 (t, J = 6.1 Hz, 2H, CH_3C-(CH_2)-$CO_2CH_2CH_2SO_3$), 4.10 (t, J = 7.0 Hz, 2H, NCH_2), 3.74 (s, 3H, NCH_3), 3.16 (t, J = 6.1 Hz, 2H, CH_3C-(CH_2)-$CO_2CH_2CH_2SO_3$), 2.85−2.75 (m, 2H, N-$(CH_2)_3CH_2SO_3H$), 1.94−1.82 (m, 2H, N-$(CH_2)_2CH_2CH_2SO_3H$), 1.77 (d, J = 0.9 Hz, 3H, CH_3C-(CH_2)-$CO_2CH_2CH_2SO_3$), 1.65−1.54 (m, 2H, $NCH_2CH_2CH_2CH_2SO_3H$); ^{13}C NMR (101 MHz, D_2O) δ 169.3 (CH_3C-$(CH_2)CO_2CH_2CH_2SO_3$), 135.9 (C-2), 135.6 (CH_3C-(CH_2)-$CO_2CH_2CH_2SO_3$), 127.0 (CH_3C-(CH_2)-$CO_2CH_2CH_2SO_3$), 123.6 (C-5*), 122.1 (C-4*), 60.0 (CH_3C-(CH_2)-$CO_2CH_2CH_2SO_3$), 50.0 (N-$(CH_2)_3CH_2SO_3$), 49.5 (CH_3C-(CH_2)-$CO_2CH_2CH_2SO_3$), 48.8 (NCH_2), 35.6 (NCH_3), 28.0 (NCH_2CH_2), 20.8 (N-$(CH_2)_2CH_2$), 17.2 (CH_3C-(CH_2)-$CO_2CH_2CH_2SO_3$); ESI-MS m/z (%) 219.07986 ($[C_8H_{15}N_2SO_3]^+$, calcd. for $C_8H_{15}N_2SO_3$ = 219.08001, 17), 437.15242 ($[(C_8H_{15}N_2SO_3)$-$(C_8H_{14}N_2SO_3)]^+$, calcd for $C_{16}H_{29}N_4O_6S_2$ = 437.15230, 100), 438.15587 ($[(C_8H_{15}N_2SO_3)$-$(C_8H_{14}N_2SO_3)$ + 1]$^+$, 17) 655.22503 ($[(C_8H_{15}N_2SO_3)$-$(C_8H_{14}N_2SO_3)_2]^+$, 33), 656.22876 ($[(C_8H_{15}N_2SO_3)$-$(C_8H_{14}N_2SO_3)_2$ + 1]$^+$, 8).

Synthesis of 1-Butylsulfonate-3-vinylimidazolium 2-Sulfethylmetacrylate. 2-Sulfethyl methacrylate (2.45 gr, 12.6 mmol, 1.00 equiv) was dissolved in CH_3CN and added over 1-butylsulfonate-3-vinylimidazolium (3.22 gr, 14 mmol, 1.10 equiv). The mixture was stirred at room temperature overnight. Then, it was filtered. The organic phase was collected, and the solvent was evaporated under reduced pressure at room temperature to avoid product decomposition. The resulting IL was dried under high vacuum to obtain 1-butylsulfonic-3-methylimidazolium 2-sulfethyl methacrylate as a viscous ionic liquid (4.85 g, 91% yield). ^{1}H NMR (400 MHz, D_2O) δ 8.96 (s, 1H, H-2), 7.67 (s, 1H, H-5*), 7.49 (s, 1H, H-4*), 7.03 (dd, J = 15.6, 8.7 Hz, 1H,, $NCH{=}CH_2$), 6.04 (s, 1H, CH_3C-(C*H*H)-$CO_2CH_2CH_2SO_3$), 5.69 (d, J = 15.6 Hz, 1H, NCH=C*H*H), 5.61 (s, 1H, CH_3C-(CH*H*)-$CO_2CH_2CH_2SO_3$), 5.31 (d, J = 8.7 Hz, 1H, NCH=CH*H*), 4.40 (t, J = 5.9 Hz, 2H, CH_3C-$(CH_2)CO_2CH_2CH_2SO_3$), 4.18 (t, J = 7.0 Hz, 2H, NCH_2), 3.19 (t, J = 5.9 Hz, 2H, CH_3C-(CH_2)-$CO_2CH_2CH_2SO_3$), 2.84 (t, J = 7.5 Hz, 2H, N-$(CH_2)_3CH_2SO_3H$), 2.01−1.89 (m, 2H, N-$(CH_2)_2CH_2CH_2SO_3H$), 1.81 (s, 3H, CH_3C-(CH_2)-$CO_2CH_2CH_2SO_3$), 1.72−1.59 (m, 2H, $NCH_2CH_2CH_2CH_2SO_3H$); ^{13}C NMR (101 MHz, D_2O) δ 169.3 (CH_3C-(CH_2)-$CO_2CH_2CH_2SO_3$), 135.6 (C-2), 134.4 (CH_3C-(CH_2)-$CO_2CH_2CH_2SO_3$), 128.2 (C-5*), 127.0 (CH_3C-(CH_2)-$CO_2CH_2CH_2SO_3$), 122.8 (C-4*), 119.5 ($NCH{=}CH_2$), 109.3 ($NCH{=}CH_2$), 60.0 (CH_3C-(CH_2)-$CO_2CH_2CH_2SO_3$), 50.0 (N-$(CH_2)_3CH_2SO_3$), 49.5 (CH_3C-(CH_2)-$CO_2CH_2CH_2SO_3$), 49.2 (NCH_2), 27.9 (NCH_2CH_2), 20.8 (N-$(CH_2)_2CH_2$), 17.2 (CH_3C-(CH_2)-$CO_2CH_2CH_2SO_3$); ESI-MS m/z (%) 231.08 ($[C_9H_{15}N_2SO_3]^+$, 8), 461.15 ($[(C_9H_{15}N_2SO_3)$-$(C_9H_{14}N_2SO_3)]^+$, 100), 462.15 ($[(C_9H_{15}N_2SO_3)$-$(C_9H_{14}N_2SO_3)$ + 1]$^+$, 17), 463.15 ($[(C_9H_{15}N_2SO_3)$-$(C_9H_{14}N_2SO_3)$ + 2]$^+$, 8), 691.22 ($[(C_9H_{15}N_2SO_3)$-$(C_9H_{14}N_2SO_3)_2]^+$, 19), 692.22 ($[(C_9H_{15}N_2SO_3)$-$(C_9H_{14}N_2SO_3)$-2 + 1]$^+$, 5).

Procedure for the Synthesis of 1-Butylsulfonate-3-Methylimidazolium Vinylphosphonate.

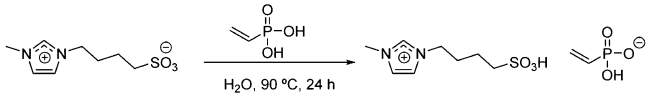

Vinylphosphonic acid (10 mL, 122.6 mmol, 1.00 equiv) was added dropwise under inert atmosphere over a solution of 1-butylsulfonate-3-methylimidazolium (26.7 g, 122.6 mmol, 1.00 equiv) in deionized water (50 mL). The mixture was stirred at 90 °C overnight. Then, solvent was evaporated under reduced pressure, and the resulting IL was washed with diethyl ether. Residual solvent was eliminated under reduced pressure, and the IL was dried by heating at 50 °C under high vacuum for 12 h. 1-Butylsulfonate-3-methylimidazolium vinylphosphonate was obtained as a colorless viscous liquid (48.0 g, 99%). ^{1}H NMR (400 MHz, D_2O) δ 8.66 (s, 1H, H-2), 7.41 (m, 1H, H-5*), 7.35 (m, 1H, H-4*), 6.26−5.88 (m, 3H, $CH_2{=}CHPO_3H$), 4.16 (t, 2H, J = 7.1 Hz, NCH_2), 3.80 (s, 3H, NCH_3), 2.86 (m, 2H, N-$(CH_2)_3CH_2$), 1.94 (m, 2H, NCH_2CH_2), 1.66 (m, 2H, N-$(CH_2)_2CH_2$); ^{13}C NMR (101 MHz, D_2O) δ 135.8 (C-2), 133.5 ($CH_2{=}CHPO_3H$), 127.4 (d, $J_{(C,P)}$ = 176.8 Hz, $CH_2{=}CHPO_3H$), 123.5 (C-5), 122.0 (C-4), 50.0 (N-$(CH_2)_3CH_2$), 48.8 (NCH_2), 35.6 (NCH_3), 28.0 (NCH_2CH_2), 20.8 (N-$(CH_2)_2CH_2$); ^{31}P NMR (162 MHz, D_2O) δ 13.87; ESI-MS m/z (%) 219.07925 ($[C_8H_{15}N_2SO_3]^+$, calcd. for $C_8H_{15}N_2SO_3$ = 219.07979, 100), 220 ($[(C_8H_{15}N_2O_3S)$ + 1]$^+$, 8), 545 ($[(C_8H_{15}N_2SO_3)_2(C_2H_4O_3P)]^+$, 21).

General Procedure for the Polymerization of Protic Ionic Liquids. Protic ionic liquids were polymerized with UV light. For this purpose, ionic liquid monomers were mixed with 5 wt % of photoinitiator 2-hydroxy-2-methyl propiophenone and 5 wt % of cross-linker glycerol dimethacrylate to improve the mechanical stability. The mixture was extended over a flat and flexible surface and exposed to 354 nm UV light (KAIS) for 30 min. After polymerization, the polymer was removed from the surface using a razor blade.

Determination of pK_a of Protic Ionic Monomers. For pK_a determinations in triplicate, a stock solution (0.01 mol/L) of the complex was prepared in degassed water. The solution was then titrated with aqueous KOH solution (0.100 mol/L). The pH of the solution was measured using a calibrated glass electrode on a Metrohm 780 pH meter at 295.0 K. The pK_a for each compound was calculated by the procedure described by Albert and Serjeant.[27]

NMR Characterization. The ^{1}H and ^{13}C NMR spectra of the purified products were recorded in D_2O on a Bruker ARX at 400.1621 (^{1}H) and 100.6314 (^{13}C) MHz. Chemical shifts are given in ppm, and coupling constants (J) are given in hertz (Hz). Data for ^{1}H NMR are reported relative to D_2O (δ 4.79 ppm). ESI mass spectra were recorded on an apex-Qe spectrometer. All spectral data were supplied by the Centre of Research Support (CACTI) of the University of Vigo.

Dielectric Measurements. Isobaric dielectric measurements at ambient pressure from 10^{-1} to 10^6 Hz were carried out using a Novocontrol GMBH Alpha dielectric spectrometer. For the isobaric measurements, the sample was placed between two stainless steel electrodes of the capacitor with a gap of 0.1 mm. The dielectric spectra of polyILs were collected over a wide temperature range. The temperature was controlled by the Novocontrol Quattro system with the use of a nitrogen gas cryostat. Temperature stability of the samples was 0.1 K. For the pressure dependent dielectric measurements, the capacitor filled with the studied samples was placed in the high-pressure chamber and compressed using the silicone oil. Note that during the measurement, the samples were in contact with stainless steel and Teflon. Pressure was measured by the Nova Swiss tensometric pressure meter with a resolution of 0.1 MPa. The temperature was controlled within 0.1 K by means of a liquid flow provided by a Weiss fridge and Julabo thermal bath. The general scheme of the apparatus used to investigate the properties of polyILs under high pressure conditions is presented in ref 29. The dielectric experimental data for poly-BuVIm TFSI were taken from ref 23.

Calorimetric Measurements. Calorimetric measurements of the studied materials were carried out by using a Mettler-Toledo DSC apparatus equipped with a liquid nitrogen cooling accessory and a

DOI: 10.1021/acs.chemmater.7b01658
Chem. Mater. XXXX, XXX, XXX−XXX

HSS8 ceramic sensor (a heat flux sensor with 120 thermocouples). Temperature and enthalpy calibrations were performed using indium and zinc standards. Using a stochastic temperature-modulated differential scanning calorimetry (TMDSC) technique, the dynamic behavior of the glass−liquid transition of the studied materials was analyzed in the frequency range from 4 to 40 mHz in a single measurement at a heating rate of 0.5 K/min. In these experiments, the temperature amplitude of the pulses of 0.5 K was selected.

Procedure of Water Content Evaluation in ILs. The protic polyIL samples were prepared in an open aluminum crucible (40 μL) outside the DSC apparatus. Next, several calorimetric measurements in the temperature range of 223−523 K at the heating rate of 10 K/min under dry nitrogen purge (60 mL/min) were performed. Each measurement was finished with a 5 min long isothermal scan of the sample at a temperature of 523 K to remove water residue. The examined material was weighed before each measurement, and the content of water remaining in the sample was determined. The above procedure was repeated until the polymer mass and T_g value had become stable. The determined water content in the examined polymer membranes is presented in the Table 1. The obtained results are in good agreement with the water content estimated from TGA analysis.

NMR Relaxometry Studies. The ^{1}H spin−lattice relaxation data were collected by a STELAR fast field cycling (FFC) relaxometer in the frequency range of 10 kHz to 25 MHz at 283, 288, 294, and 303 K. The data are shown in the Supporting Information (Figure S1).

DFT Calculations. DFT calculations were used to determine the pK_a of acids and bases used to prepare protic ionic samples. The calculations were performed in water environment; therefore, the pK_a values are related to the situation when the proton is solvated by water. The G-(A^-) and G-(AH) energies were calculated using the Orca 4 program.[28] The geometry optimizations of all acids and related bases were done on the B3LYP/6-311G-(2d,2p) level of theory. For final energy evaluation, PBE0 gradient functional and 6-311G-(2d,2p) basis set was used. The solvent model CPCM was used during optimization and energy evaluation run. Vibrational, thermal, and entropic corrections were evaluated on the B3LYP/6-311G-(2d,2p) level of theory. The energy of a proton was calculated analytically based on literature values. Free energy of proton used in the calculations was equal to −270.29 kcal/mol.

RESULTS

Sample Characterization. The materials examined herein were designed as model systems to understand the molecular mechanism of charge transport in polymerized ionic liquids. We can classify them into three categories: protic polyanions, aprotic polycations, and polymer blends composed of cations and anions covalently attached to the polymer chains.

The first group is represented by imidazolium-based polycations with mobile TFSI anion and cations covalently attached to the polymer chain. Such chemical design favors a single ion conductivity in these polyILs. The second group of polyILs studied herein includes two novel polyanions with the chemical moieties promoting proton transport. Specifically, the butylimidazolium cation terminated by the sulfonate group (SBIm) was chosen to create two Brønsted pairs with sulfethylmetacrylate (SEM) and vinylphosphonic poly acids, respectively. There are at least two reasons to justify this selection. First, the chemical structure of the sulfobuthylimidazolium cation has the potential to favor proton hopping in ionic systems. It is well-known that the terminal acidic groups SO_3H located in the side chains of polymer electrolyte membranes such as Nafion exposed to water dissociate into immobile SO_3^- anions and free protons that move through the hydrogen-bonded network thereby are responsible for the high conductivity of the system. Likewise, of great importance is vinylphosphonic acid, due to the highly efficient Grotthuss mechanism confirmed in phosphoric acid. Furthermore, sulfethyl methacrylate anion was chosen to duplicate the amount of proton acceptor groups in SBMIm SEM system, which could result in enhancement in conductivity. Another great advantage of SEM is the possibility of formation of a structure of polymer blend with complex architecture that is advantageous for fundamental understanding of the parameters affecting conductivity. In the poly-SBVIm poly-SEM system, where both cations and anions are covalently bonded to two different vinyl chains, the structural reorganization is strongly suppressed. This, together with the fact that there are no other freely mobile ions besides OH^- and H_3O^+, has resulted in the development of novel material with pure proton conductivity. This is in contrast to polyanions mentioned above where the SBMIm cation also contributes to dc conductivity, and thus, it is difficult to unambiguously recognize the dominating charge transport mechanism.

To analyze the ability of the studied materials to attach/detach protons, we performed DFT calculations of the SBMIm cation, SEM, and vinyl-HPO_3 anions. The SEM demonstrates the strongest acidity with pK_a = −2.16. Slightly weaker acid properties is present in SBMIm with pK_a = −1.42, while vinylHPO_3 is a very weak acid with first pK_{a1} equal to 9.02. It should be noted that the strong interactions, e.g., hydrogen bonds between polar groups in polyanions, can change the pK_a value. Therefore, influence of hydrogen bonds on pK_a of dimers has been also studied. In case of SBMIm, an additional conformation with the SO_3H group in the close vicinity of the imidazole ring has been also evaluated (see Table 1 in Supporting Information). We found that acidity of vinyl-HPO_3 dimers is suppressed, i.e. the pK_a value is increasing from 9.02 to 13.94. The increase in the acidity has been found in the SEM dimer (pK_a decreases from −2.16 to −4.76) as well as in the SBMIm compound. For the conformation C2 of SBMIm, pK_a has been changed from −1.42 to −4.56. Very low values of pK_a found for both SEM and SBMIm ions suggest that the proton can be easily dissociated. Furthermore, terminal HSO_3 groups in cations exposed to water can also generate protons. Consequently, SEM-based polymer membranes are a mixture of imidazolium-based zwitterions (being mobile in SBMIm poly-SEM and linked to the alkyl chain in polymer blend), poly-SO_3^- anions, and H_3O^+. On the other hand, high pK_a value of HPO_3 suggests that the protons are likely transferred from SBMIm to polyanion and are not moving along the polymer chains. As a result, the water saturated SBMIm poly-HPO_3 membrane is composed mostly of zwitterions, neutral poly-H_2PO_3 structure, and water molecules that strongly participate in proton transport.

To characterize materials, we employed TGA and calorimetric measurements. The DSC scans obtained during heating of all polymerized ILs are presented in Figure 1. As can be seen, the DSC curves of polyILs reveal heat flow jump, which is a characteristic of the liquid−glass transition. The exact values of T_g are listed in Table 2. Because the examined protic polyILs are water saturated, in the thermograms, one can also observe broad endotherms related to the water evaporation. However, it can be easily discerned that in SBMIm polyHPO_3, this effect is less pronounced compared to that in two other protic polyILs with lower water content. The water fraction in the examined protic polyILs was determined by the weight difference between not-dried and dried sample (see the Experimental Section for details). We found that the sulfethylmetacrylate-based polyILs contain 13.8 wt % of water, while the material with the poly-HPO_3 group is characterized by a water content equal to 11 wt %.

DOI: 10.1021/acs.chemmater.7b01658
Chem. Mater. XXXX, XXX, XXX−XXX

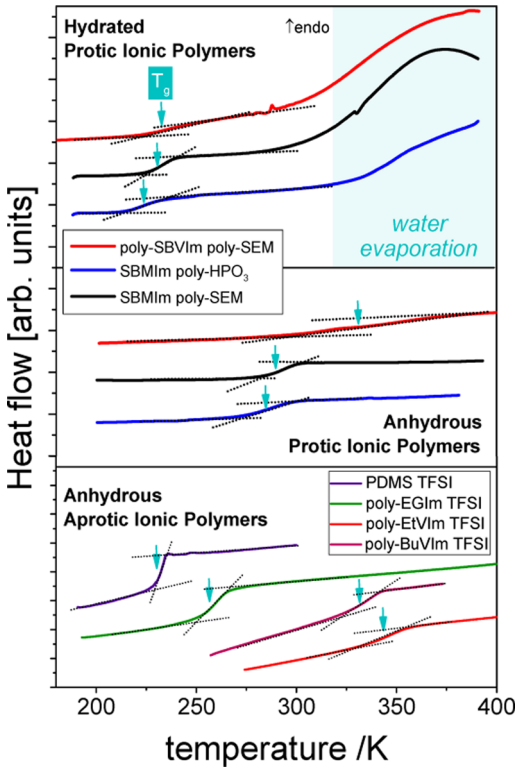

Figure 1. DSC curves of polyILs. The green arrows indicate the liquid−glass transition of given system.

From Figure 1, the glass transition for anhydrous membranes is 60−70 K higher compared to that of hydrated samples.

In contrast to protic polyILs, special care was taken to remove any water from TFSI conductors. Before the measurements, the samples were extensively dried in a vacuum oven at temperature above 393 K for 3−4 days. Additionally, in the DSC system, polyILs were further preconditioned at ∼393 K for 30−60 min in nitrogen atmosphere to remove surface water. Several heating−cooling scans were performed to ensure that both T_g of a sample and its mass do not change. As presented in the Figure 1, the obtained DSC scans of aprotic ionic liquids studied herein reveal only liquid−glass transition without any sign of the presence of water.

Dielectric Data at Ambient Pressure. In general, the dielectric experiments performed in the external electric field with frequency interval of milli- to megahertz and a wide temperature range, covering the supercooled liquid regime as well as glassy state, enables a thorough analysis of relaxation dynamics of any macromolecular system. For most conventional polymers, valuable insight into segmental relaxation and local intramolecular motions can be obtained from dielectric loss $\varepsilon''(f)$ spectra. However, if the molecular dynamics are strongly dominated by translational displacement of charge carrying species or proton transport, as observed for polyILs, dc conductivity gives rise to a sharp increase in the dielectric loss function and completely masks the relaxation of polymer segments. Therefore, information obtained from dielectric studies of polyILs is limited to conductivity behavior.

The most convenient approach to define conductivity contribution to dielectric response and thereby to characterize the translational motions of charge carriers in the studied material is related to analysis of complex electric modulus, $M^*(f) = M'(f) + iM''(f) = 1/\varepsilon^*(f)$ and electric conductivity $\sigma^*(f) = \sigma'(f) + \sigma''(f)$ formalisms.[29,30] The dielectric data of SBMIm polySEM are presented in Figure 2.

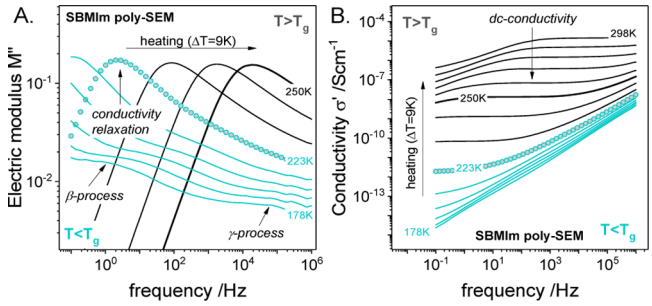

Figure 2. Dielectric loss modulus (A) and conductivity (B) spectra of SBMIm polySEM recorded over a wide temperature range. Spectrum recorded at T_g is denoted by circles.

As can be seen, the imaginary part of modulus function $M''(f)$ has the form of a well-resolved asymmetric peak, the so-called conductivity relaxation peak ascribed to the translational ionic motions. On the other hand, two clearly visible regions characterize the real part of the complex conductivity spectra: the power law behavior observed at higher frequencies and frequency-independent plateau that corresponds to the dc conductivity σ_{dc}. Note that σ_{dc}, directly related to the number of free ions and their mobility, is inversely proportional to the conductivity relaxation times τ_σ estimated from the frequency of M'' peak maximum $\tau_\sigma = \varepsilon_0\varepsilon_s/\sigma_{dc} = {}^1/_{2\pi f_{max}}$, where ε_s is static permittivity.[29,30]

Typically, the position of the modulus peak maximum (as well as dc conductivity) is strongly dependent on thermodynamic conditions, i.e., σ-mode moves toward lower frequencies with cooling/squeezing and approaches $f \approx 0.15$ mHz ($\tau_\sigma \approx$ 1000 s) at the liquid−glass transition, if only the ion transport is fully controlled by viscosity, like in the case of classical low-molecular ILs. However, as can be clearly seen in Figure 2, $M''(f)$

Table 2. Characteristics of PolyILs Used in This Study[a]

polyILs	T_{dec} (K)	T_g (K)	σ_{dc} at 300 K (S/cm)	σ_{dc} at T_g (S/cm)	R (T_g)
poly-SBVIm poly-SEM	529	229	9.5×10^{-6}	9×10^{-11}	5
SBMIm poly-SEM	533	224	2.5×10^{-5}	4.7×10^{-12}	3.8
SBMIm poly-HPO3		224	5.5×10^{-6}	9×10^{-13}	3
poly-EtVIm TFSI	520	344	2.9×10^{-11}	1.7×10^{-9}	6.5
poly-BuVIm TFSI		335	9.1×10^{-11}	1.7×10^{-9}	6.5
poly-EGIm TFSI	551	259	3.9×10^{-7}	1.5×10^{-11}	4
PDMS TFSI	417	233	4.6×10^{-5}	7.4×10^{-14}	2

[a] T_g, glass transition temperature (from DSC, heating rate 10 K/min); *T_g of hydrated sample; T_{dec} decomposition temperature obtained from TGA measurements; σ_{dc} dc conductivity; R (T_g) decoupling index calculated at T_g.

DOI: 10.1021/acs.chemmater.7b01658
Chem. Mater. XXXX, XXX, XXX−XXX

of SBMIm poly-SEM collected at T_g appears at frequencies markedly higher than f_{max} of ideally coupled systems.

Additionally, from Figure 3A, it appears that the $M''(f)$ spectra of all studied herein polyILs recorded at their

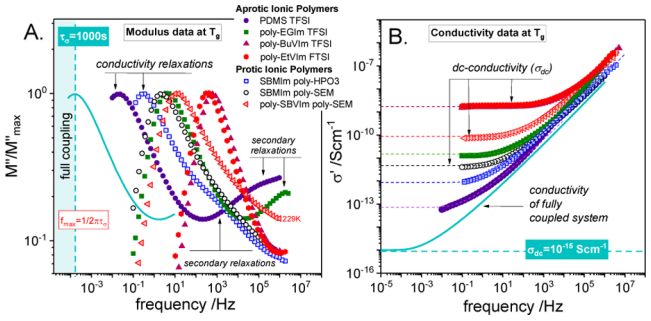

Figure 3. Dielectric loss modulus (A) and conductivity (B) spectra of seven polyILs measured at their calorimetric T_g. The dotted lines in panel B are fit of the conductivity data to the Dyre model.[31] The solid lines show spectra expected for systems with ion dynamics strongly coupled to segmental relaxation.

calorimetric T_g cover the frequency range of about five decades, and importantly, none of them is close to the frequency expected for a coupled system (solid line). At the same time, in each examined case, the $\sigma_{dc}(T_g)$ is higher than 10^{-15} S cm^{-1}: the value typical for ionic conductors with the charge transport strongly coupled to structural relaxation (see Figure 3B). These are the first signs that generally the rate of charge diffusion is different than the motions of polymer segment and specifically that the efficiency of this process is changing among examined samples. Nevertheless, to characterize the ion dynamics in more detail, the dielectric data of all polymers tested herein both in the supercooled liquid regime as well as in the glassy state need to be analyzed.

The temperature dependences of conductivity relaxation time of all seven polyILs exhibit qualitatively similar behavior (Figures 4A and B), i.e. a well-defined crossover from the Vogel–Fulcher–Tamman (VFT) to Arrhenius-like behavior at the glass transition temperature T_g, being a typical behavior observed in ionic systems.[6,32,33] More importantly, $\tau_\sigma(T_g)$ differs in studied polyILs, but in all cases, it is faster than 10^2 to 10^3 s usually identified with the freezing point of the structural/segmental relaxation at T_g. The direct comparison between the results of temperature modulated DSC experiments (see stars

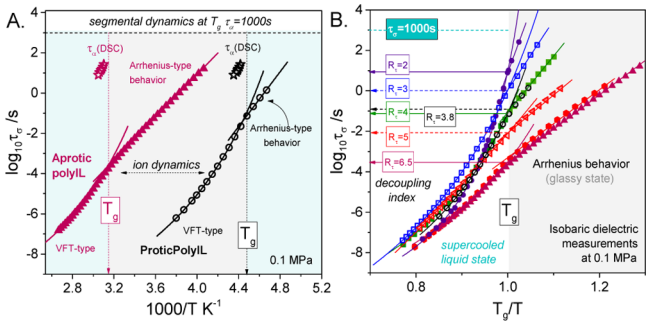

Figure 4. Conductivity relaxation times determined from $M''(f)$ spectra, presented vs 1000/T for polyBuVIm TFSI and SBMIm poly-SEM (A) and vs T_g/T for all studied polyILs (B). Open stars are τ_α data determined from TM DSC technique. Symbol presents the same samples as those in Figure 3A.

in Figure 4A), representing the time scale of segmental dynamics, and conductivity relaxation data clearly indicate that the ion diffusion is significantly faster than the rate of segmental motions at T_g in studied polyILs. According to many studies, a simple way to quantify the decoupling of charge diffusion from structural relaxation in the vicinity of the glass transition temperature is to calculate the decoupling index defined as $R_\tau(T_g) = 3 - \log\tau_\sigma(T_g)$.[14,15,34]

Importantly, the time scale separation between τ_σ and τ_α is also reflected in the conductivity behavior. In Figure 5, σ_{dc} data

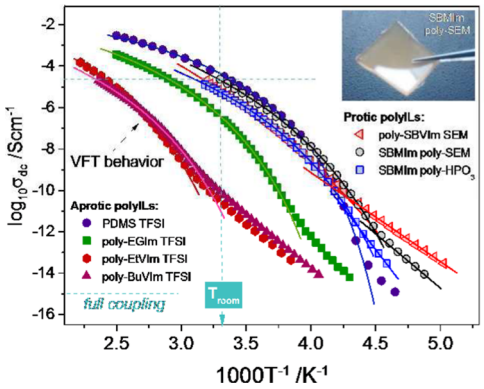

Figure 5. Temperature dependence of dc conductivity for protic and aprotic polyILs determined by means of BDS technique.

taken directly from the frequency independent part of $\sigma'(f)$, are plotted as a function of inverse temperature. As can be seen, $\sigma_{dc}(T_g)$ is significantly higher than expected for coupled systems ~10^{-14} to 10^{-15} S/cm, and the difference is similar to that reported between τ_σ and τ_α. The values of σ_{dc} measured at T_g of all polyILs investigated in this paper are listed in Table 2.

Among the studied polyILs, PDMS TFSI shows the highest value of dc conductivity at room temperature conditions (Figure 5). The σ_{dc} around 5×10^{-5} S cm^{-1} obtained at 303 K most likely results from the combination of the low T_g of the siloxane backbone and highly delocalized, noncoordinating and asymmetric TFSI anion. Interestingly, the room temperature conductivity of studied protic polyILs is also high (see Table 2), even in the case of polymer blend, where only fast proton transfer is expected to give contribution to charge transport.

Dielectric Data at Elevated Pressure. According to the standard experimental protocol, all polyILs were compressed isothermally at several different temperatures above the calorimetric T_g. Although both modulus $M''(f)$ and conductivity $\sigma'(f)$ formalisms provide the same information about the ion dynamics (Figures 3 and 4), the former enables a more accurate analysis close to the liquid–glass transition, and therefore, it was chosen for use in presenting the high pressure data for polyILs. The representative high pressure results are depicted in Figure 6. It is apparent that isothermal compression has basically the same effect on ion dynamics as isobaric cooling. Namely, the conductivity relaxation times τ_σ of supercooled polyILs are getting longer with squeezing and markedly slow down when a material solidifies. Consequently, the experimental points exhibit two linear regimes that intersect at the glass transition pressure, P_g. Interestingly, the markedly lower pressure sensitivity is evident for τ_σ of hydrated membranes. This agrees with the general rule, indicating that systems with well-expanded H-bonded network are characterized by weaker sensitivity to a compression.[35] The further inspection of high

DOI: 10.1021/acs.chemmater.7b01658
Chem. Mater. XXXX, XXX, XXX–XXX

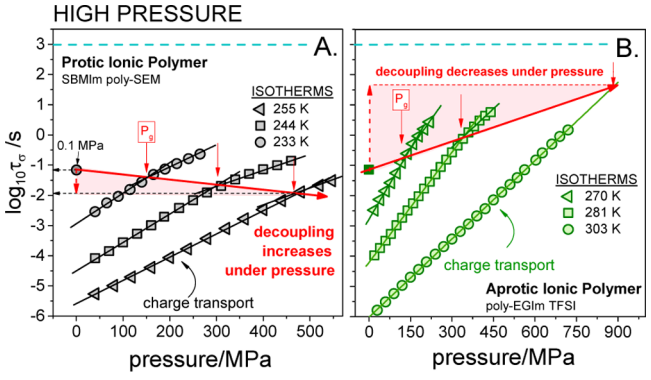

Figure 6. Pressure dependence of ion dynamics. Panels A and B present the pressure behavior of conductivity relaxation times measured at isothermal conditions for protic and aprotic ionic polymers, respectively. The single experimental point at log-(τ_σ) ~ −1 indicates the value of $\tau_\sigma(T_g)$ recorded at 0.1 MPa.

pressure conductivity relaxation data reveals some universal features of ion dynamics in tested polyILs. Namely, it is evident that the value of conductivity relaxation time at the inflection point, being a manifestation of the glass transition, is continuously changing with pressure. This fact, together with the recent report demonstrating that regardless of $T-P$ thermodynamic conditions the characteristic crossover of log-(τ_σ) occurs at isochronal structural relaxation time ($\tau_\alpha \approx 10^3$s),[36] indicates that compression strongly affects the decoupling between τ_σ and τ_α in the studied polyILs.

As presented in Figure 6 and summarized in Figure 7, the application of pressure as an external thermodynamic variable makes the $\tau_\sigma(P_g)$ faster in protic ionic polymers and thus enhances the time scale separation between charge transport and segmental dynamics in these systems. However, in the cases of TFSI-based materials, isothermal compression brings the crossover of log-(τ_σ)-(P) to longer conductivity relaxation times, and thereby, the decoupling between τ_σ and τ_α becomes markedly reduced under pressure. Interestingly, at high enough pressure, the time scales of charge transport and segmental

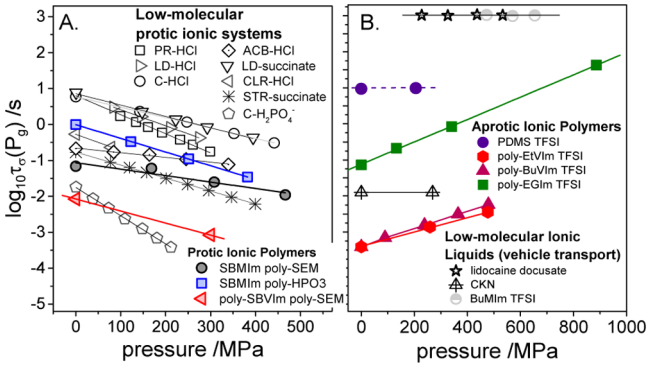

Figure 7. Panels A and B present the pressure variations of τ_σ measured at P_g of protic and aprotic ionic polymers, respectively (closed symbols). In addition, the results of another 11 low-molecular ionic systems were taken from literature (open symbols). Abbreviations are as follows: prilocaine HCl (PR-HCl),[37] lidocaine HCl (LD-HCl),[38] carvedilol HCl (C-HCl),[45] acebutolol HCl (ACB-HCl),[36] lidocaine succinate (LD-SUCC), chlorpromazine HCl (CLR-HCl), Sumatriptan succinate (STR SUCC),[39] carvedilol dihydrogen phosphate (C−$H_2PO_4^-$),[45] lidocaine docusate, Ca-$(NO_3)_2$-KNO_3 (CKN),[40,41] butylmethyl imidazole TFSI (BuMIm TFSI).[42]

dynamics became practically coupled, as it is shown for poly-EGIm TFSI at ~1 GPa. These results stand in sharp contrast with the behavior of PDMS TFSI, where the time scale of conductivity relaxation is almost the same as for segmental dynamics. In this special case, compression of the sample up to 200 MPa does not affect $\tau_\sigma(P_g)$, and ion dynamics remains coupled to segmental dynamics.

DISCUSSION

To provide the physical explanation for experimental results, one needs to consider the charge transport mechanism in all of the studied polymerized ionic liquids. From the chemical point of view, polyILs (except for the polymer blend) can be treated as single-ion conductors due to the only one type of freely moving ion (TFSI anion or SBIm cation). As a consequence, the origin of the decoupling phenomenon can be ascribed to the different contribution of cations and anions to the ionic conductivity and segmental relaxation. Namely, the motions of charged polymeric segments are expected to govern segmental dynamics, but at the same time, these are too slow to provide significant contribution to σ_{dc}. The latter parameter is dominated by the diffusion of counterions, presumably through free volume associated with frustration in polymer chain packing. As a consequence of such an assumption, any reduction of free volume, including compression-induced, should result in slowing of charge transport at the same segmental relaxation time and hence increase τ_σ at P_g. However, the experimental data collected in Figure 7 clearly demonstrates that only three of seven polyILs follow this assumption: these are BuVIm, EtVIm, and EGIm polycations with TFSI counterion dominating charge transport. Interestingly, the PDMS-based polyIL with the same TFSI counterion exhibits the smallest decoupling, consistent with the expectation that the most flexible chain (siloxane-based) should reveal better packing and lower free volume. Moreover, in this particular case, the decoupling appears to be independent of $T-P$ conditions (Figure 7B), again consistent with the idea of free volume controlling the decoupling.

Most important, in contrast to aprotic polyILs, an increase in pressure strongly accelerates $\tau_\sigma(P_g)$ in all water saturated membranes. This result clearly demonstrates a significant difference in conductivity mechanisms between aprotic polyILs and hydrated protic polyILs: it reveals that translational diffusion of free ions is no longer crucial and suggests that an effective proton transfer is involved in charge transport of examined water saturated polymer membranes. This is because only the proton transfer speeds up when hydrogen bond length decreases[43] and the H-bonded network is stressed,[44] both taking place under high pressure conditions. An additional argument emerges from the recent studies of low molecular weight protic ionic liquids and solids, showing that $\tau_\sigma(P_g)$ becomes faster under high pressure only if the conductivity is governed by a fast proton transfer mechanism.[45] The comparison of high pressure data for low-molecular and macromolecular ionic systems is presented in Figure 7.

Surprisingly, there is no correlation between the value of the decoupling index at ambient conditions and its pressure dependence. For example, the HPO_3-based protic polyIL with relatively small time scale separation between τ_σ and τ_α at ambient conditions exhibits a very strong change in decoupling under elevated pressure (Figure 7A). Furthermore, despite the fact that $R_\tau(T_g)$ is smaller for poly-(EGIm)-TFSI than in poly-(EtVIm)-TFSI and poly-(BuVIm)-TFSI, it reduces in the

DOI: 10.1021/acs.chemmater.7b01658
Chem. Mater. XXXX, XXX, XXX−XXX

similar way with pressure (Figure 7B). Interestingly, the lack of correlation between $R_\tau(T_g)$ and its pressure behavior can be also found for low-molecular ionic systems.

To further advance our understanding of high pressure behavior of decoupling phenomena, we focus on two variables that quantify the pressure sensitivity of both charge transport and glass transition temperature. These are pressure coefficient of decoupling index $d\log\text{-}(R_\tau)/dP = d\log\text{-}(\tau)\text{-}(P_g)/dP$ and pressure coefficient of glass transition temperature dT_g/dP, both calculated at 0.1 MPa. As illustrated in Figure 8, the

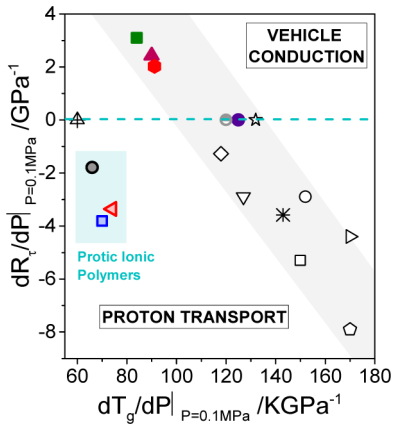

Figure 8. Pressure coefficient of decoupling index as a function of dT_g/dP (for procedure of dT_g/dP ,calculation see ref 33). The dashed line presents fully coupled systems and divides the examined materials into two categories of dominating conductivity mechanism: proton transfer ($dR_\tau/dP < 0$) and free volume controlled ($dR_\tau/dP \geq 0$).

studied herein polyILs (except PDMS TFSI) are characterized by relatively low values of dT_g/dP parameter (70−90 KGPa^{-1}); markedly lower than those found for low-molecular ionic conductors (see Figure 7) and nonionic polymers.[46] These results reflect weak pressure sensitivity of segmental dynamics that can be explained in terms of poor packing of vinyl backbones under pressure as well as the expanded H-bonded network in PEMFCs. Despite the fact that generally T_g of polyILs does not increase much with squeezing, the substantial changes in charge transport are observed for these systems under pressure (the absolute value of dR_τ/dP is between 2 and 4 per GPa). This creates a possibility to obtain polymerized ionic liquids with super protonic properties directly by isothermal compression. This is in contrast to low-molecular weight protic ILs where an efficient proton mobility under pressure can be achieved only for systems with large value of dT_g/dP coefficient.

Interestingly, due to the large value of the decoupling index at ambient pressure conditions ($R_\tau(T_g) = 5$) and significant change of τ_σ accompanying squeezing, the polymer blend (poly-SBVIm poly-SEM) can be regarded as the most efficient proton conductor among the herein studied protic systems over a wide $T-P$ thermodynamic space. Because both cations and anions are covalently attached to rigid vinyl chains, the structural reorganization is strongly suppressed in this system. As a consequence, the H-bonds are not prone to breaking and can be treated as highways for fast proton transport. The idea of efficient proton migration in a polymer blend is also supported by experimentally determined ΔpK_a values. Among the tested protic polyILs, SBVIm SEM structure reveals the smallest $\Delta pK_a = 1.17$ and thereby the lowest free energy of proton dissociation. On the other hand, the largest value of ΔG (corresponding to the highest $\Delta pK_a = 2.11$) characterizes proton transport of the HPO_3-based compound. Poor proton dissociation in this system is consistent with the dielectric data, revealing the smallest decoupling index for SBMIm poly-HPO_3 at ambient pressure.

This clearly demonstrates that dielectric studies, especially under conditions of high compression, are ideal experimental tools for empirical verification of the dominating conductivity mechanism in ionic systems in general. However, at the same time, it should be noted that from dielectric measurements it is difficult to separate contribution of proton motions and simple vehicle transport to overall dc conductivity. Nevertheless, knowing the temperature behavior of conductivity relaxation times τ_σ and the "jump" length λ of ions, one can employ the Random Barrier Model (RBM) $D = \lambda^2/6\tau_\sigma$ to calculate diffusivity (D) that reflects the translational motions of all conducting species in the studied material. Note that RBM provides a good agreement between D parameter estimated by BDS and measured by NMR for various aprotic IL and polymerized ionic liquids.[47] Therefore, to provide more insight into charge transport in studied protic systems, we used SBMIm HPO_3 monomer as a model compound and compared the translational diffusion coming from NMR relaxometry studies and D_{RBM} calculated from BDS data. The obtained NMR results are presented in the Supporting Information and summarized in Table 3.

Table 3. Parameters Obtained from the Analysis of ^{1}H Spin−Lattice Relaxation Data for SBMIm HPO_3 Monomer

T (K)	λ (Å)	D_{trans}[a] (m^2 s^{-1})	D_{RBM} (m^2 s^{-1})
283	2.95	6.64×10^{-13}	8.93×10^{-12}
288	2.89	1.0×10^{-12}	1.36×10^{-11}
294	2.86	1.03×10^{-12}	1.83×10^{-11}
303	2.82	2.66×10^{-12}	3.19×10^{-11}

[a]Because there were no significant differences between D_{trans} of cations and anions, the presented values denote $2D_{trans}$ of cations.

Herein, it should be noted that the NMR results for λ, being in good agreement with values reported by Sangoro et al.[48] for other ILs, were used to calculate D_{RBM}. Interestingly, we found at least one order of magnitude difference between NMR and BDS diffusivity coefficients. Namely, D_{trans}, reflecting only the translational diffusion of SBMIm cations and vinylHPO_3 anions, is slower than D_{RBM}. Because both vehicle conduction and proton motions were found to contribute to the dielectric relaxation data, one can expect that the observed difference between D_{trans} and D_{RBM} comes from proton hopping between the conducting species. Taking into account that the value of the decoupling index was found to be practically the same for SBMIm HPO_3 monomer and polymer (see Figure 3 in Supporting Information), with a similar activation energy for charge transport in the glassy state, one can assume that proton motions give similar contribution to dc conductivity in both of these compounds. Consequently, D_{RBM} is expected to be faster than D_{trans} also in SBMIm poly-HPO_3.

Another interesting aspect of ion dynamics in protic polyILs is the effect of water on the decoupling between segmental and ionic relaxation. To investigate this issue, we performed additional dielectric measurements of dry SBMIm poly-SEM membrane. As can be clearly seen in Figure 9, evaporation of water results in dramatic increase in T_g (68 K) accompanied by

DOI: 10.1021/acs.chemmater.7b01658
Chem. Mater. XXXX, XXX, XXX−XXX

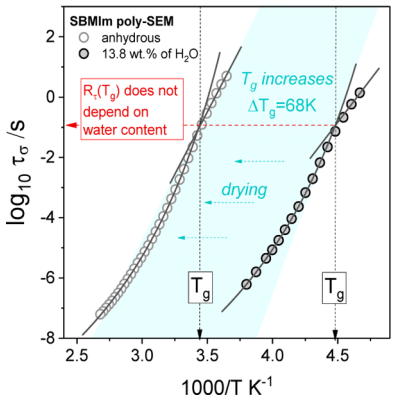

Figure 9. Conductivity relaxation times presented vs $1000/T$ for SBMIm poly-SEM. Open symbols are τ_α data for the anhydrous sample.

decrease in dc conductivity; however, at the same time, the crossover of log-(τ_σ)-$(1/T)$ dependence occurs at the same conductivity relaxation time. This result clearly indicates that at the liquid−glass transition the charge transport in the annealed protic polyIL is still faster than the segmental dynamics and consequently, the conducting properties of the examined dried polymer are still governed by the fast proton hopping through the H-bond network. These results are consistent with the data obtained for other protic polyILs published in ref 17.

From a closer look at Figure 9, one can also see that the apparent activation energies determined for conductivity relaxation in the glassy state of anhydrous and hydrated material differ from each other. Namely, it is a little higher for the dried sample. This indicates that below T_g when the segmental dynamics is completely frozen, it is more difficult for proton to hop through the dry material. That can be very easily explained in terms of the amount of proton active sites, which is continuously decreased with the decrease in water content.

CONCLUSIONS

The studies of seven protic and aprotic polymerized ionic liquids combined with literature data for 11 low-molecular ionic systems have revealed the great potential of high pressure dielectric techniques for developing fundamental understanding of the conductivity mechanism in ionic glass-formers in general. It has been demonstrated that the characteristic crossover of $\tau_\sigma(P_g)$ appears at shorter relaxation times with elevating pressure for proton conducting systems. This observation suggests a dominating proton transfer mechanism in newly synthesized hydrated protic polyILs that becomes even more efficient under compression due to shortening and stressing of H-bonds. On the other hand, the opposite behavior, i.e. a decrease in decoupling, was found in aprotic ionic polymers. These results confirm the dominating role of the chain packing and free volume in charge transport of aprotic systems. As a consequence, isothermal compression offers a unique possibility to recognize the dominating charge transport mechanisms as well as control the conducting properties of polyILs, both being crucial in their potential electrochemical applications. Additionally, the high decoupling between segmental dynamics and ion transport found in poly-SBVIm poly-SEM demonstrates that polymer blends in general provide a possibility to design polyILs with exceptionally high proton conductivity and satisfactory mechanical stability.

ASSOCIATED CONTENT

Supporting Information

The Supporting Information is available free of charge on the ACS Publications website at DOI: 10.1021/acs.chemmater.7b01658.

Details of NMR relaxometry measurements, DFT calculations, and dielectric data of monomer SBMIm vinylHPO3 (PDF)

AUTHOR INFORMATION

Corresponding Author

*E-mail: zaneta.wojnarowska@smcebi.edu.pl.

ORCID

Zaneta Wojnarowska: 0000-0002-7790-2999
Hongbo Feng: 0000-0002-8806-6041
Justyna Knapik-Kowalczuk: 0000-0003-3736-8098
Emilia Tojo: 0000-0002-7099-3437
Tomonori Saito: 0000-0002-4536-7530
Nam-Goo Kang: 0000-0003-3492-9080
Vera Bocharova: 0000-0003-4270-3866

Notes

The authors declare no competing financial interest.

ACKNOWLEDGMENTS

Z.W., J.K-K. and M.P. are deeply grateful for the financial support by the National Science Centre within the framework of the Opus8 project (Grant DEC-2014/15/B/ST3/04246). This work was supported by Laboratory Directed Research and Development program of Oak Ridge National Laboratory, managed by UT-Battelle, LLC, for the U.S. Department of Energy. J.W.M. and A.P.S. acknowledge partial financial support for help with synthesis and data analysis/interpretation by the U.S. Department of Energy, Office of Science, Basic Energy Sciences, Materials Sciences, and Engineering Division. E.T. is grateful to the Xunta de Galicia (REGALIs Network R2014/015) for their financial support as well as the research support services of the University of Vigo (CACTI) for the NMxR and MS divisions work. M.D., A.O., and I.O. acknowledge the Spanish Ministry of Economy and Competitiveness for Project CTQ2015-66078-R (MINECO/FEDER, UE) and the Project "PEMFC-SUDOE"-SOE1/P1/E0293 which is co-financed by the FEDER in the framework of the "Interreg Sudoe programme". M.D. is grateful to the Spanish Ministry of Education, Culture and Sport for Project FPU2012-3721.

REFERENCES

(1) Armand, A.; Endres, F.; MacFarlane, D. R.; Ohno, H.; Scrosati, B. Ionic-liquid materials for the electrochemical challenges of the future. *Nat. Mater.* **2009**, *8* (8), 621−629.

(2) Bruce, D. W.; O'Hare, D. I. W. R. *Energy Materials*, 1st ed.; Wiley: Hoboken, NJ, 2011.

(3) Xu, W.; Angell, C. A. Solvent-free electrolytes with aqueous solution-like conductivities. *Science* **2003**, *302*, 422−425.

(4) MacFarlane, D. R.; Forsyth, M.; Howlett, P. C.; Kar, M.; Passerini, S.; Pringle, J. M.; Ohno, H.; Watanabe, M.; Yan, F.; Zheng, W.; Zhang, S.; Zhang, J. Ionic liquids and their solid-state analogues as materials for energy generation and storage. *Nature Reviews Materials* **2016**, *1*, 15005.

(5) Sangoro, J. R.; Kremer, F. Charge transport and glassy dynamics in ionic liquids. *Acc. Chem. Res.* **2012**, *45*, 525−32.

(6) Choi, U. H.; Ye, Y. S.; de la Cruz, D. S.; Liu, W. J.; Winey, K. I.; Elabd, Y. A.; Runt, J.; Colby, R. H. Dielectric and Viscoelastic

DOI: 10.1021/acs.chemmater.7b01658
Chem. Mater. XXXX, XXX, XXX−XXX

Responses of Imidazolium-Based Ionomers with Different Counterions and Side Chain Lengths. *Macromolecules* **2014**, *47* (2), 777−790.
(7) Nakamura, K.; Fukao, K. Dielectric relaxation behavior of polymerized ionic liquids with various charge densities. *Polymer* **2013**, *54* (13), 3306−3313.
(8) Sangoro, J. R.; Iacob, C.; Agapov, A. L.; Wang, Y.; Berdzinski, S.; Rexhausen, H.; Strehmel, V.; Friedrich, C.; Sokolov, A. P.; Kremer, F. Decoupling of ionic conductivity from structural dynamics in polymerized ionic liquids. *Soft Matter* **2014**, *10*, 3536−3540.
(9) Choi, U. H.; Mittal, A.; Price, T. L., Jr; Lee, M.; Gibson, H. W.; Runt, J.; Colby, R. H. Molecular Volume Effects on the Dynamics of Polymerized Ionic Liquids and their Monomers. *Electrochim. Acta* **2015**, *175*, 55−61.
(10) Frenzel, F.; Folikumah, M. Y.; Schulz, M.; Anton, A. M.; Binder, W. H.; Kremer, F. Molecular Dynamics and Charge Transport in Polymeric Polyisobutylene-Based Ionic Liquids. *Macromolecules* **2016**, *49* (7), 2868−2875.
(11) Fan, F.; Wang, W.; Holt, A. P.; Feng, H.; Uhrig, D.; Lu, X.; Hong, T.; Wang, Y.; Kang, N.-G.; Mays, J.; Sokolov, A. P. Effect of Molecular Weight on the Ion Transport Mechanism in Polymerized Ionic Liquids. *Macromolecules* **2016**, *49*, 4557−4570.
(12) Fan, F.; Wang, Y.; Hong, T.; Heres, M. F.; Saito, T.; Sokolov, A. P. Ion Conduction in Polymerized Ionic Liquids with Different Pendant Groups. *Macromolecules* **2015**, *48* (13), 4461−4470.
(13) Mizuno, F.; Belieres, J. P.; Kuwata, N.; Pradel, A.; Ribes, M.; Angell, C. A. Highly decoupled ionic and protonic solid electrolyte systems, in relation to other relaxing systems and their energy landscapes. *J. Non-Cryst. Solids* **2006**, *352*, 5147−5155.
(14) Angell, C. A. Dynamic Processes in Ionic Glasses. *Chem. Rev.* **1990**, *90*, 523−542.
(15) Ingram, M. D. Ingram Ionic conductivity and glass structure. *Philos. Mag. B* **1989**, *60* (6), 729−740.
(16) Díaz, M.; Ortiz, A.; Ortiz, I. Progress in the use of ionic liquids as electrolyte membranes in fuel cells. *J. Membr. Sci.* **2014**, *469*, 379−396.
(17) Wojnarowska, Z.; Knapik, J.; Diaz, M.; Ortiz, A.; Ortiz, I.; Paluch, M. Conductivity mechanism in polymerized imidazolium-based protic ionic liquid [HSO3−BVIm]-[OTf]: dielectric relaxation studies. *Macromolecules* **2014**, *47*, 4056−65.
(18) Kim, S. Y.; Kim, S.; Park, M. J. Enhanced proton transport in nanostructured polymer electrolyte/ionic liquid membranes under water-free conditions. *Nat. Commun.* **2010**, *1*, 88.
(19) Angell, C. Dynamic processes in ionic glasses. *Chem. Rev.* **1990**, *90*, 523−542.
(20) Mangiatordi, F. G.; Butera, V.; Russo, N.; Laage, D.; Adamo, C. Charge transport in poly-imidazole membranes: a fresh appraisal of the Grotthuss mechanism. *Phys. Chem. Chem. Phys.* **2012**, *14*, 10910−10918.
(21) Wojnarowska, Z.; Paluch, K. J.; Shoifet, E.; Schick, C.; Tajber, L.; Knapik, J.; Wlodarczyk, P.; Grzybowska, K.; Hensel-Bielowka, S.; Verevkin, S. P.; Paluch, M. Molecular origin of enhanced proton conductivity in anhydrous ionic systems. *J. Am. Chem. Soc.* **2015**, *137* (3), 1157−1164.
(22) Kang, S. D.; Snyder, G. J. Charge-transport model for conducting polymers. *Nat. Mater.* **2016**, *16*, 252.
(23) Wojnarowska, Z.; Knapik, J.; Jacquemin, J.; Berdzinski, S.; Strehmel, V.; Sangoro, S. R.; Paluch, M. Effect of pressure on decoupling of ionic conductivity from segmental dynamics in polymerized ionic liquids. *Macromolecules* **2015**, *48*, 8660−8666.
(24) Wojnarowska, Z.; Feng, H.; Fu, Y.; Cheng, S.; Kumar, R.; Novikov, V. N.; Kisliuk, A.; Saito, T.; Kang, N.; Mays, J.; Sokolov, A. P.; Bocharova, V. Effect of chain rigidity on the decoupling of ion motion from segmental relaxation in polymerized ionic liquids: Ambient and elevated pressure studies. *Macromolecules* **2017**, *50*, 6710.
(25) Jeong, Y.; Kim, D. Y.; Choi, Y.; Ryu, J. S. Intramolecular hydroalkoxylation in Brønsted acidic ionic liquids and its application to the synthesis of (±)-centrolobine. *Org. Biomol. Chem.* **2011**, *9*, 374−378.
(26) Zhou, H.; Song, Z.; Kang, X.; Hu, J.; Yang, Y.; Fan, H.; Meng, O.; Han, B. One-pot conversion of carbohydrates into gamma-valerolactone catalyzed by highly cross-linked ionic liquid polymer and Co/TiO2. *RSC Adv.* **2015**, *5*, 15267−15273.
(27) Albert, A.; Serjeant, E. P. *The Determination of Ionization Constants: A Laboratory Manual*, 3rd ed.; Chapman and Hall: New York, 1984.
(28) Neese, F. The ORCA program system, Wiley interdisciplinary Rev. *Comp. Mol. Sci.* **2012**, *2*, 73.
(29) Paluch, M. *Dielectric properties of ionic liquids*; Springer: Berlin, 2016.
(30) Kremer, F., Schoenhals, A. *Broadband Dielectric Spectroscopy*; Springer: Berlin, 2003.
(31) Dyre, J. C.; Maass, P.; Roling, B.; Sidebottom, D. L. Fundamental questions relating to ion conduction in disordered solids. *Rep. Prog. Phys.* **2009**, *72*, 046501.
(32) Wojnarowska, Z.; Roland, C. M.; Swiety-Pospiech, A.; Grzybowska, K.; Paluch, M. Anomalous electrical conductivity behavior at elevated pressure in the protic ionic liquid procainamide hydrochloride. *Phys. Rev. Lett.* **2012**, *108*, 015701.
(33) Wojnarowska, Z.; Paluch, M. Recent progress on dielectric properties of protic ionic liquids. *J. Phys.: Condens. Matter* **2015**, *27*, 073202.
(34) Hodge, I. M.; Ngai, K. L.; Moynihan, C. T. Comments on the electric modulus function. *J. Non-Cryst. Solids* **2005**, *351*, 104.
(35) Roland, C. M.; Casalini, R.; Bergman, R.; Mattsson, J. Role of hydrogen bonds in the supercooled dynamics of glass-forming liquids at high pressures. *Phys. Rev. B: Condens. Matter Mater. Phys.* **2008**, *77*, 012201.
(36) Wojnarowska, Z.; Rams-Baron, M.; Knapik, J.; Połatyńska, A.; Pochylski, M.; Gapinski, J.; Patkowski, A.; Paluch, M. Experimental evidence of high pressure decoupling between charge transport and structural dynamics in protic ionic glass-former. *Sci. Rep.* **2017**, 1.
(37) Wojnarowska, Z.; Roland, C. M.; Swiety-Pospiech, A.; Grzybowska, K.; Paluch, M. Anomalous electrical conductivity behavior at elevated pressure in the protic ionic liquid procainamide hydrochloride. *Phys. Rev. Lett.* **2012**, *108*, 015701 DOI: 10.1103/PhysRevLett.108.015701.
(38) Swiety-Pospiech, A.; Wojnarowska, Z.; Pionteck, J.; Pawlus, S.; Grzybowski, A.; Hensel-Bielowka, S.; Grzybowska, K.; Szulc, A.; Paluch, M. High pressure study of molecular dynamics of protic ionic liquid lidocaine hydrochloride. *J. Chem. Phys.* **2012**, *136*, 224501.
(39) Wojnarowska, Z.; Knapik, J.; Rams-Baron, M.; Jedrzejowska, A.; Paczkowska, M.; Krause, A.; Cielecka-Piontek, J.; Jaworska, M.; Lodowski, P.; Paluch, M. *Mol. Pharmaceutics* **2016**, *13* (3), 1111−1122.
(40) Paluch, M.; Wojnarowska, Z.; Hensel-Bielowka, S. Heterogeneous Dynamics of Prototypical Ionic Glass CKN Monitored by Physical Aging. *Phys. Rev. Lett.* **2013**, *110*, 1.
(41) Wojnarowska, Z.; Ngai, K. L.; Paluch, M. Invariance of conductivity relaxation under pressure and temperature variations at constant conductivity relaxation time in 0.4Ca-(NO3)-2−0.6KNO3. *Phys. Rev. E* **2014**, *90*, 062315.
(42) Wojnarowska, Z.; Jarosz, G.; Grzybowski, A.; Pionteck, J.; Jacquemin, J.; Paluch, M. On the scaling behavior of electric conductivity in [C4mim]-[NTf2]. *Phys. Chem. Chem. Phys.* **2014**, *16*, 20444−50.
(43) Kreuer, K. D. On the complexity of proton conduction phenomena. *Solid State Ionics* **2000**, *136−137*, 149−160.
(44) Vilciauskas, L.; Tuckerman, M. E.; Bester, G.; Paddison, S. J.; Kreuer, K. D. The mechanism of proton conduction in phosphoric acid. *Nat. Chem.* **2012**, *4*, 461−6.
(45) Wojnarowska, Z.; Wang, Y.; Pionteck, J.; Grzybowska, K.; Sokolov, A. P.; Paluch, M. High pressure as a key factor to identify the conductivity mechanism in protic ionic liquids. *Phys. Rev. Lett.* **2013**, *111*, 225703.
(46) Roland, C. M.; Hensel-Bielowka, S.; Paluch, M.; Casalini, R. Supercooled dynamics of glass-forming liquids and polymers under hydrostatic pressure. *Rep. Prog. Phys.* **2005**, *68*, 1405.

DOI: 10.1021/acs.chemmater.7b01658
Chem. Mater. XXXX, XXX, XXX−XXX

(47) Gainaru, C.; Stacy, E. W.; Bocharova, V.; Gobet, M.; Holt, A. P.; Saito, T.; Greenbaum, S.; Sokolov, A. P. Mechanism of Conductivity Relaxation in Liquid and Polymeric Electrolytes: Direct Link between Conductivity and Diffusivity. *J. Phys. Chem. B* **2016**, *120*, 11074−11083.
(48) Sangoro, J. R.; Iacob, C.; Naumov, S.; Valiullin, R.; Rexhausen, H.; Hunger, J.; Buchner, R.; Strehmel, V.; Karger, J.; Kremer, F. Diffusion in Ionic Liquids: the Interplay Between Molecular Structure and Dynamics. *Soft Matter* **2011**, *7*, 1678−1681.

DOI: 10.1021/acs.chemmater.7b01658
Chem. Mater. XXXX, XXX, XXX−XXX